Journal of Electroceramics 2:1, 21–31, 1998

Synthesis, Microstructure and Electrical Properties of Hydrothermally Prepared Ferroelectric $BaTiO_3$ Thin Films

W. ZHU

Department of Materials Science and Engineering, Center for Integrated Systems Development, Semiconductor Product Sector, Motorola, Inc., Mail Drop: AE100, Phoenix, AZ 85008

S.A. AKBAR

Department of Materials Science and Engineering, Center for Industrial Sensors and Measurements (CISM), 291 Watts Hall, The Ohio State University, 2041 College Road, Columbus, OH 43210, e-mail akbar.1@osu.edu

R. ASIAIE

Department of Chemistry, the Ohio State University, Columbus, OH 43210
Department of Chemical Engineering, Yale University, New Haven, CT 06520

P.K. DUTTA

Department of Chemistry, The Ohio State University, Columbus, OH 43210

Received September 17, 1996; Revised October 2, 1997; Accepted October 14, 1997

Abstract. Thin films of polycrystalline, tetragonal $BaTiO_3$ on oxidized Ti metal substrates were synthesized at 240°C under hydrothermal conditions. Microstructure and electrical properties of the films generated over a four week period of synthesis formed the focus of this study. The films displayed a smooth and shiny surface with a relatively dense structure and no observable cracks. Film thickness reached 0.5 μm after two weeks of synthesis and thereafter remained constant. Diameters of the grains on the film surface were in the range of $1 \sim 2\,\mu$m. It is proposed that initial formation of the $BaTiO_3$ film occurs by reaction of Ba^{2+} with solubilized titanium oxide on the Ti metal surface followed at later stages by an in-situ growth via reaction of TiO_x with Ba^{2+} diffusing through the $BaTiO_3$ film. X-ray diffraction and Raman spectroscopy indicated that the $BaTiO_3$ films are tetragonal, and the films exhibited typical ferroelectric hysteresis loops at room temperature. However, no evidence of the dielectric anomaly (Curie transition) between 30 and 200°C was observed. Dielectric constant of the films at 1 kHz at room temperature was between 400–500. Both dielectric constant and $tan\delta$ exhibited low dispersion as a function of frequency at temperatures below 150°C, and the dispersion increased with temperature.

Keywords: barium titanate, $BaTiO_3$, ceramics, ferroelectric thin films, hydrothermal synthesis

Introduction

Recent advances in thin film processing technologies have led to a renewed interest in ferroelectric thin films for potential applications in areas such as large-volume thin-film capacitors [1], optical waveguide devices [2], and non-volatile semiconductor memories [3]. Barium titanate ($BaTiO_3$) with a relatively large dielectric constant and electro-optic coefficient, is an attractive candidate for these applications.

There has been substantial effort in improving the processing and properties of ferroelectric thin films. The common methods for $BaTiO_3$ thin film synthesis include thermal evaporation [4], *rf* and magnetron sputtering [5], metal-organic chemical vapor deposition (MOCVD) [6–7] and sol-gel method [8–11].

These preparation techniques often require high temperature annealing (usually $> 800°C$) for crystallization, which may cause problems such as chemical reactions between the film and the substrate, or cracks in the film due to a large difference in thermal expansion coefficients between the film and the substrate.

The hydrothermal method [12–24] has been recently used as a promising technique for processing of ferroelectric thin films. It allows preparation of crystalline films directly at low temperatures (typically less than 100°C) without the need of post-deposition annealing. With only slight modifications of the powder synthesis, films with high purity and grain sizes in submicron range can be prepared. However, the films usually display a non-ferroelectric cubic structure at room temperature with low dielectric constants ($100 \sim 200$), though the stable phase of $BaTiO_3$ single crystal at room temperature is tetragonal and ferroelectric with dielectric constant above 1000.

In this study, hydrothermal conditions were used to directly synthesize tetragonal $BaTiO_3$ thin films at a relatively low temperature (240°C). The microstructural evolution of the films with time of synthesis, as well as the electrical properties of the films as a function of temperature and frequency were examined. We have previously reported on hydrothermal synthesis of $BaTiO_3$ powders using reactants of TiO_2 gel, barium chloride and sodium hydroxide [25–26]. We report here the extension of this methodology to the synthesis of tetragonal $BaTiO_3$ thin films and evaluation of their structural and electrical properties.

Experimental Section

The procedure used previously for $BaTiO_3$ powder synthesis was modified for film formation [26]. $BaCl_2$ (99.999%, Johnson Matthey) was used as the barium source. Titanium foils (99.99 + %, Johnson Matthey) of $3 \times 3\,cm^2$ in area and 0.25 mm in thickness were used as the substrates as well as the titanium source. The Ti foils were surface polished with alumina to a 0.05 μm finish and cleaned ultrasonically in acetone. They were then etched in 6 M HCl, and subsequently oxidized in a calcination chamber at 500°C under flowing oxygen for 12 h. The oxidized Ti plates were then washed with water before the synthesis.

The synthesis was performed in a 23 mL Teflon-lined acid digestion bomb (Parr Instrument Co.). 0.002 mol of $BaCl_2 \cdot 2H_2O$ was dissolved in 10 mL of boiled water (i.e., $[Ba^{2+}] = 0.2$ M). The oxidized Ti foils were then placed in the solution. To minimize the formation of any carbonate species, nitrogen gas was bubbled into the solution during the addition of 0.01 mol of NaOH into the solution (i.e., $[OH^-] = 1.0$ M). The bomb was immediately sealed and placed in the oven at 240°C for various periods of time (1–4 weeks).

Room-temperature X-ray diffraction was performed using a powder X-ray diffractometer (model PAD-V, Scintag). The XRD patterns were collected using Cu*Ka* radiation at a voltage and current of 45 kV and 20 mA, respectively. X-ray diffraction at temperatures from 45 to 200°C was done using a hot-stage X-ray diffractometer (model HT-PAD, Scintag) at a scanning rate of 0.1°/min from 44 to 46° (2θ).

The microstructure and morphology of the $BaTiO_3$ films were examined using scanning electron microscope (model SL-30, Phillips) with an EDS (energy dispersive spectroscopy) detector for elemental analysis. Raman spectra of all the samples at room temperature were obtained using an Ar ion laser (model 171, Spectra-Physics, 514.5 nm, 50 mW) as the excitation source.

The electrical properties of the synthesized films were studied both as a function of temperature and frequency using an impedance analyzer (Model 4192A, Hewlett Packard). Gold dots were deposited onto the films to form top electrodes using a mask with equi-distant holes of $1\,mm^2$ in area via vacuum-evaporation. The titanium substrate acted as a counter electrode. The films were placed on the platinum coated surface of a hot chuck, which controlled the sample temperature from room temperature to 300°C with 0.1°C accuracy. The electrical measurement was performed with the help of a probe station (MC Systems) using two probes with a metal-insulator-metal (MIM) configuration. The electrical measurements as a function of temperature were performed at two fixed frequencies, 1 kHz and 100 kHz. Samples were examined during both heating and cooling cycles. Measurements during the cooling cycle involved heating of the film to 220°C, maintaining the temperature for 30 min (to remove any surface-adsorbed water), and the measurements were taken as the sample was cooled with a rate of 1°C/min. The frequency dependent electrical measurement involved recording the parallel capacitance (C_P) and conduc-

tance (G_P) were recorded over the frequency range from 5 Hz to 13 MHz. Hysteresis measurement was done using a standardized ferroelectric tester (RT66A, Radiant Technologies). The breakdown strength of the films were measured by applying the dc bias voltage on the films and continually increasing it until the films reached the breakdown level. The room temperature dc resistivity of the films were measured using a Keithley 6517 electrometer.

Results

The titanium source in this study was a titanium oxide film grown on the surface of a Ti metal plate by oxidation with oxygen at 500°C. XRD of the oxidized Ti foil only showed peaks due to Ti indicating that the oxidized layer was amorphous, which has been suggested to be TiO_{2-x} [13]. If the Ti substrate was not well polished prior to the oxidation, a second phase besides $BaTiO_3$ segregated along the grain boundaries. EDS analysis indicated that this phase is a Ti-rich barium titanate compound, which is consistent with a previous study suggesting the formation of $Ba_2Ti_9O_{20}$ [20] on unpolished substrates. All experiments reported here were done with polished Ti substrates.

A. Microstructure

The formation of $BaTiO_3$ thin films were examined as a function of synthesis time. Figure 1 illustrates the

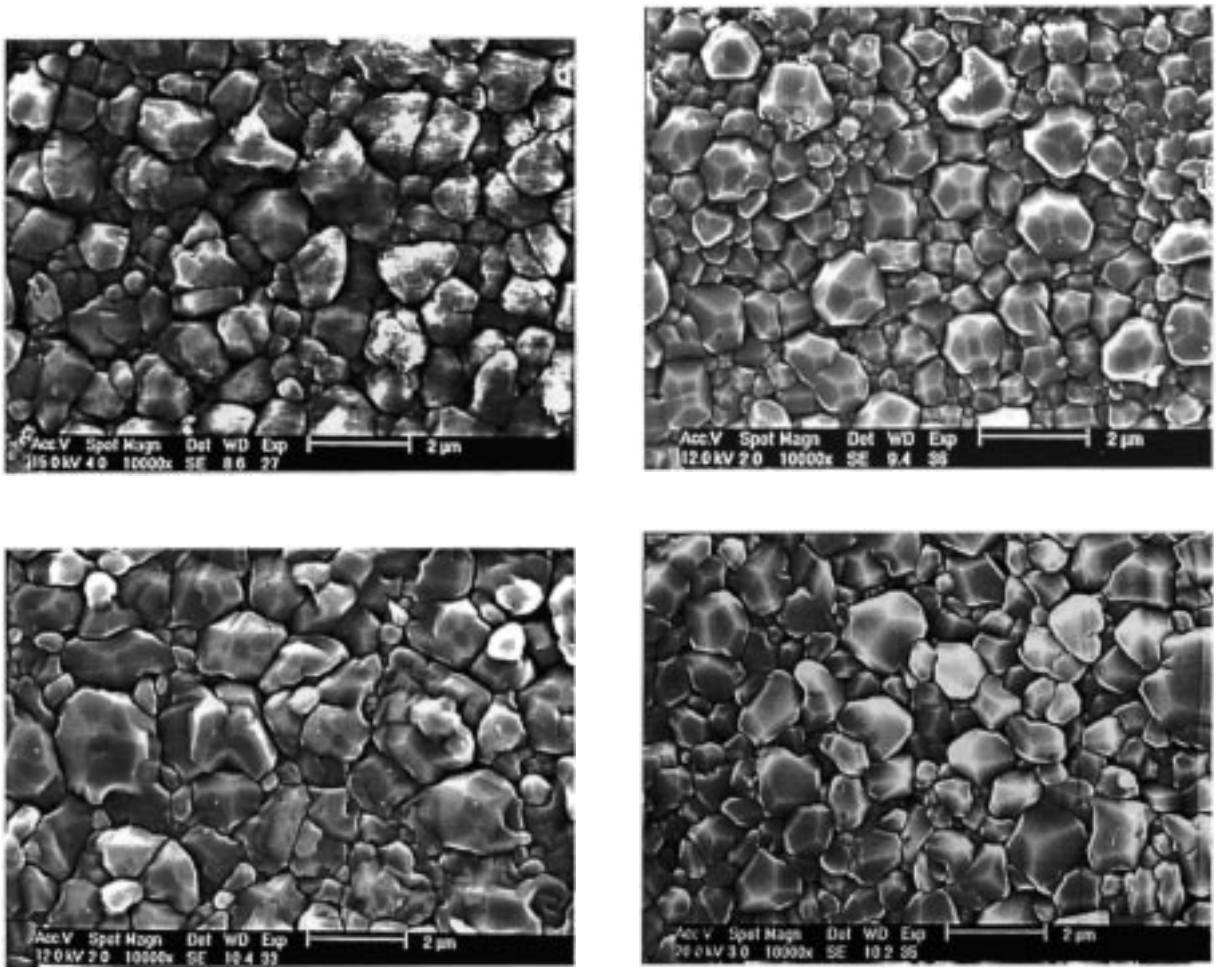

Fig. 1. SEM micrographs of the $BaTiO_3$ thin films synthesized for (a) 1 week, (b) 2 weeks, (c) 3 weeks and (d) 4 weeks.

morphology of the films synthesized for 1 to 4 weeks. Films synthesized for 1 and 2 weeks displayed irregular-shaped grains with an average size of approximately $1 \sim 2\,\mu$m. As the synthesis time exceeded 3 weeks, the grains showed more faceted surfaces. Figure 2 shows the morphology of the film (after 3 weeks of synthesis) at low magnification. The film exhibited relatively smooth and dense surface with no indication of surface cracks. No significant change in film thickness was observed beyond two weeks. Figure 3 reveals the cross-sectional view of a representative film sample synthesized for 3 weeks, with a thickness of about 0.5 μm. We ascribe this layer to $BaTiO_3$. If the TiO_x remained unreacted, it should have converted to anatase. Diffraction and Raman spectroscopy show no evidence of anatase and we believe that all of the starting TiO_x is being converted to $BaTiO_3$.

The room temperature X-ray diffraction results of the $BaTiO_3$ films recovered after different synthesis times are shown in Fig. 4. Only the diffraction peaks due to the $BaTiO_3$ film and the Ti substrate were observed. The relative intensities of the $BaTiO_3$ peaks with respect to those of the Ti substrate increased with time, suggesting improved crystallinity of the films. This may correlate with the more regular-shaped and faceted grains observed for the films synthesized for 3 and 4 weeks. The structure of the as-synthesized films were further examined by XRD between 44 and 46° (2θ) at various temperatures using a hot-statge. Figure 5 shows the diffraction patterns for a 3-week film as

Fig. 2. Low magnification SEM micrograph showing a smooth, dense and crack free surface of the $BaTiO_3$ film synthesized for 3 weeks.

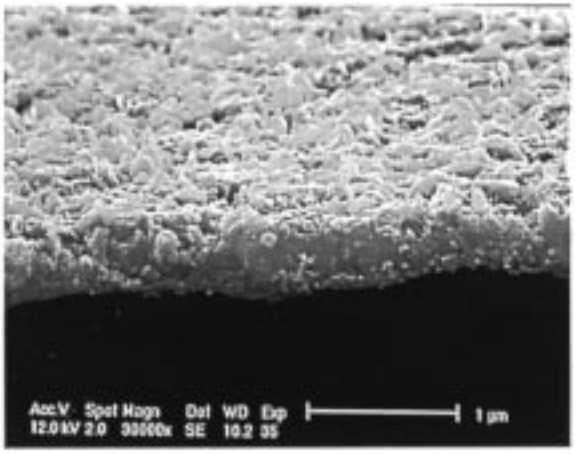

Fig. 3. SEM micrograph showing thickness of film synthesized for 3 weeks.

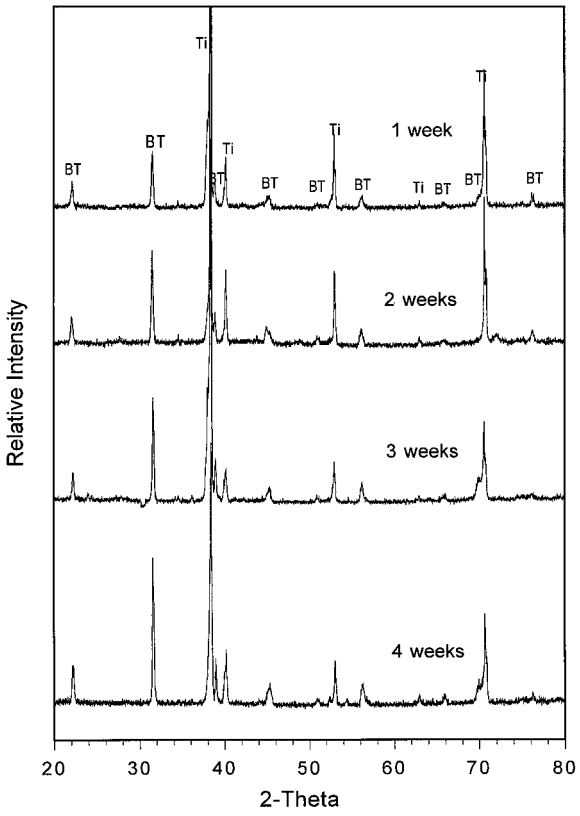

Fig. 4. Room temperature XRD patterns of the $BaTiO_3$ thin films synthesized for 1, 2, 3 and 4 weeks respectively. $BaTiO_3$ phase is indicated as BT and Ti phase as Ti.

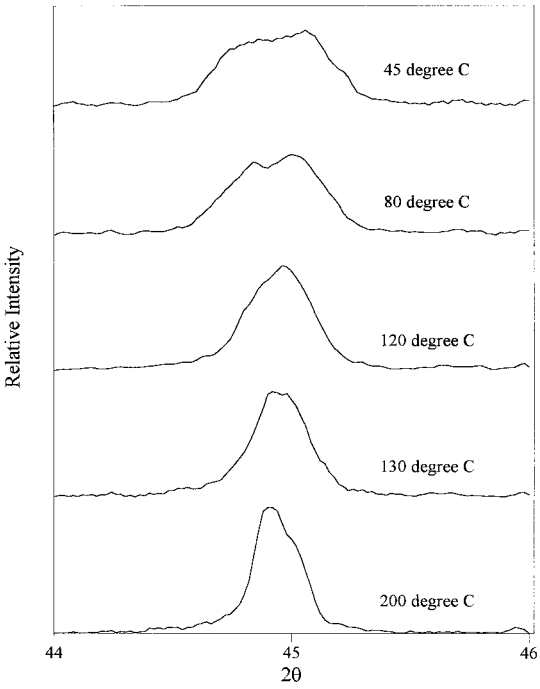

Fig. 5. XRD scans between 44 and 46°/2θ at different temperatures for the $BaTiO_3$ film synthesized for 3 weeks.

sample temperature decreased from 200 to 45°C. Transition from the cubic to tetragonal structure is evident by the evolution of double reflections (i.e., (200) and (002)) from a single (200)-type reflection. Assuming the reflection peaks are of Gaussian type, the intensity ratio of the (002) and (200) reflections (I_{002}/I_{200}) was calculated by deconvolution and peak fitting. The ratio is about 0.8 at 45°C, which is greater than that of the tetragonal $BaTiO_3$ powder ($I_{002}/I_{200} = 0.5$). This may indicate a preferred orientation of the crystals along the crystallographic *c*-axis. The reason is not clear yet; it may relate to the slightly higher surface energy of the *c*-planes (e.g., (002)) which tends to be eliminated during the film nucleation and growth processes. Similar observations were made for films synthesized for 2 and 4 weeks, suggesting that the films became tetragonal after 2 weeks of synthesis.

To further verify the tetragonal symmetry of the films, Raman spectra were performed. Figure 6 shows a typical Raman spectrum of the 3-week film. The bands observed are a weak peak around 715 cm^{-1}, two strong and broad peaks around 515 and 260 cm^{-1}, and a sharp peak at 305 cm^{-1}. The bands around 515 and 260 cm^{-1} are assigned to the TO modes of A_1 symmetry, whereas the sharp peak at 305 cm^{-1} has been assigned to the B_1 mode. The weak band around 715 cm^{-1} has been associated with the highest frequency longitudinal optical mode (LO) of A_1 symmetry. The band at 305 cm^{-1} is characteristic of $BaTiO_3$ with a tetragonal symmetry, and it disappears upon heating above the Curie temperature [26–28]. Raman study therefore also confirm that the films produced here are tetragonal $BaTiO_3$.

B. Electrical Properties

1. Temperature dependence of dielectric constant (K) *and loss tangent* (tanδ). The capacitance (*C*) and loss tangent (*tanδ*) were measured as a function of temperature for all the films, and the dielectric constant values (*K*) were calculated. The $BaTiO_3$ film synthesized for one week exhibited high loss and leakage current. It is believed to be caused by the relatively porous structure of the film, indicative of incomplete reaction. Thus, further characterization of this sample was not pursued.

Figure 7 shows the measured *K* and *tanδ* of the 3-week sample as a function of temperature measured at a frequency of 100 kHz. The data were taken from room temperature to 200°C and also upon cooling. It was found that there is a discrepancy between the heating and cooling cycles. Dependence of the capacitance of films on the thermal history of the sample has been noted before [11]. A possible cause of this effect is adsorbed moisture [11,30]. Since the adsorbed moisture evaporates upon heating, more accurate dielectric constants could be obtained during the cooling cycle. As shown in Fig. 7, *K* does not show an anomaly peak (Curie transition) that is expected around 120°C for ferroelectric $BaTiO_3$. However, the loss tangent (*tanδ*) in Fig. 7 exhibits a small peak at $\sim$120°C, indicative of a Curie transition. Figure 8 shows *K* vs. temperature plot of the 2-, 3- and 4-week samples measured at 100 kHz during the cooling cycle, and that of the 2-week sample measured at 1 kHz. Again in all these experiments, the dielectric anomaly of *K* was not observed. At room temperature, the dc resistivity of the 3-week film was measured to be about 2×10^{12} Ω-cm, and the breakdown strength of the film was around 0.8 MV/cm.

2. Ferroelectric Hysteresis. Figure 9 shows a typical ferroelectric hysteresis (*P*–*E*) loop observed at room temperature of the 3-week film. The values of

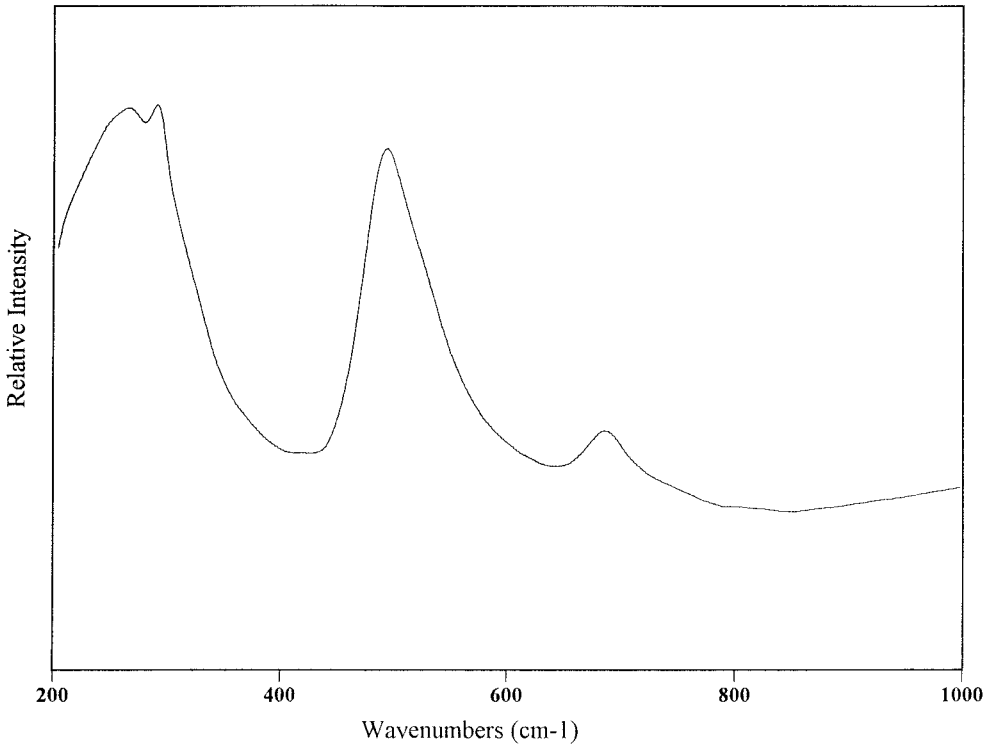

Fig. 6. Room temperature Raman spectrum of the 3-week $BaTiO_3$ film.

remnant polarization (P_r) and coercive field (E_C) are about $12\,\mu C/cm^2$ and 50 kV/cm, respectively. Although the dielectric constant does not exhibit the Curie anomaly, the hysteresis behavior shows ferroelectric characteristics.

3. Frequency dependence of dielectric constant (K) *and loss tangent* (tanδ). The electrical measurements were carried out as a function of frequency (f) at several temperatures for the 3-week film. Figure 10 shows the dielectric constant (K) and loss tangent ($tan\delta$) plotted as a function of f at three temperatures ranging from 50 to 200°C. A dispersion of K was evident at low frequencies, and the dispersion became more significant at high temperatures. Similar behavior was also observed for $tan\delta$. The low-frequency dispersion of K observed in this study is less significant as compared with those observed in previous films prepared hydrothermally [31] or by sol-gel procedures [11] measured at same temperatures.

The ac conductivity (σ_{ac}) of the 3-week film was calculated according to Eq. 1, and plotted as a function of f from 50 to 300°C in a log scale.

$$\sigma_{ac} = \sqrt{G_p^2 + (\omega C_p)^2}(t/A) \quad (1)$$

where t is the thickness of the thin film and A is the electrode area.

It was found that log (σ_{ac}) increases almost linearly with log (f) (Fig. 11). The curves are close to each other at high frequencies, with only a slight deviation taking place at the low-frequency end (< 100 Hz).

Discussion

A. Hydrothermal Synthesis

It has been shown that hydrothermal formation of microcrystalline $BaTiO_3$ usually follows a dissolution/precipitation mechanism with the dissolution of the precursors in the solution and the formation of $BaTiO_3$ as precipitate [18,19,22–24,26]. Typical chemical reactions for this process can be depicted as:

$$TiO_2 + 2H_2O \Leftrightarrow Ti(OH)_4(aq) \quad (2)$$

$$Ba^{2+} + Ti(OH)_4(aq) \Leftrightarrow BaTiO_3 + 2H^+ + H_20 \quad (3)$$

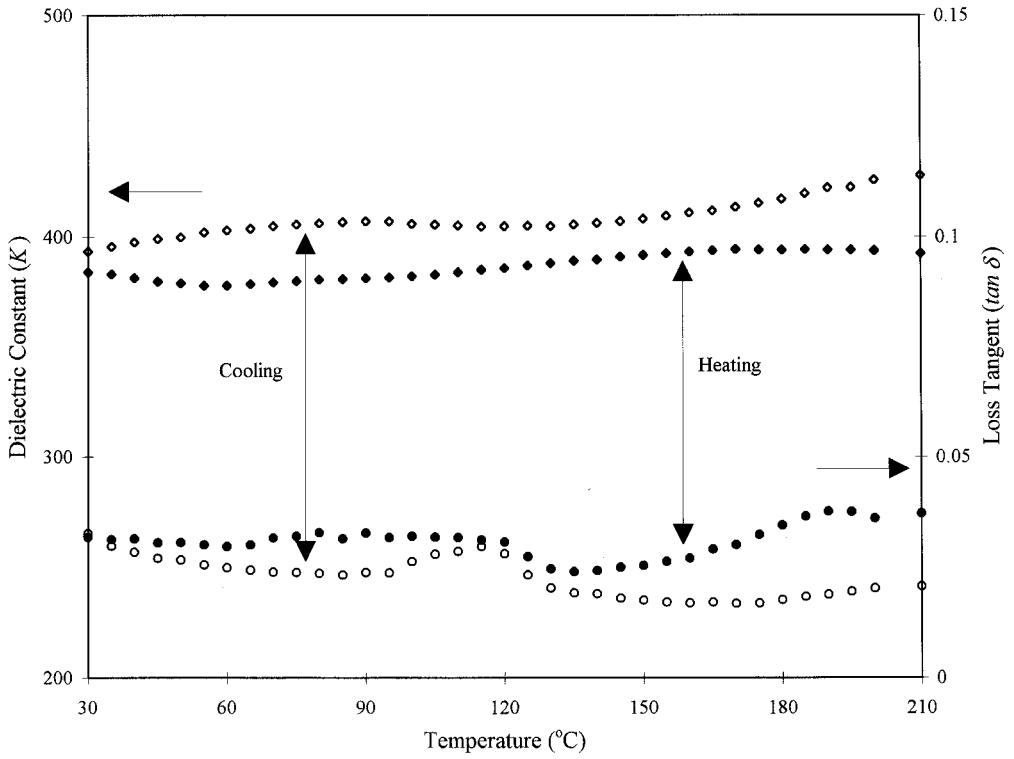

Fig. 7. Dielectric measurement results on the 2-week film at a frequency of 100 kHz from he room temperature to 200°C and subsequently cooled back to room temperature.

It is evident from the reactions that high OH^- concentration promotes $BaTiO_3$ formation, whereas lower OH^- concentrations should result in unreacted TiO_2. In this study, $[OH^-]$ of the reactant mixture is 0.5 M.

With a dissolution type mechanism, the amorphous TiO_x on the surface of the Ti substrate needs to be first hydrolyzed to form reactive intermediates such as $[Ti(OH)_4]$ [18] or $[Ti(OH)_6^{2-}]$ [12], which will then react with Ba^{2+} ions to form $BaTiO_3$ nuclei, which are subsequently deposited (adsorbed) onto the substrate surface [19,20]. This mechanism can be considered to be an example of heterogeneous nucleation via the reaction of surface adsorbed titanium species.

The nuclei on the Ti surface would grow into larger crystals at a rate dependent on the temperature and the degree of supersaturation. It is assumed that in the early stage of crystal growth, the grains grow unhindered along the substrate with a relatively rapid rate. However, as the TiO_x layer reacts completely and covers the substrate with grains coalescing with each other, a second mechanism which involves diffusion of Ba^{2+} through the porous $BaTiO_3$ will need to occur. In this case, the rate of growth would be greatly reduced. In a recent study of hydrothermal synthesis of $BaTiO_3$ from TiO_2 powders, Riman and coworkers proposed that both dissolution-precipitation and in-situ crystal growth mechanisms may be important at different stages of growth [32]. We indeed believe that this is the case in the thin film growth observed in this study.

It was also noted that the grains in the first and second week films are large and irregular in shape, whereas for the third and fourth week films, there seems to be a slight decrease in the grain size and the appearance of the faceted surface (Fig. 1). This may be caused by the local dissolution of $BaTiO_3$ as the synthesis proceeds beyond two weeks. The dissolved species may subsequently redeposit on the surface of the $BaTiO_3$ film following a ledge mechanism [21], as suggested by the faceted surfaces of the grains for the third and fourth week films.

In most previous studies, synthesis was done at temperatures between 100 and 200°C, and the formation of pseudocubic $BaTiO_3$ was observed on the film. Tetragonal films were reported only at

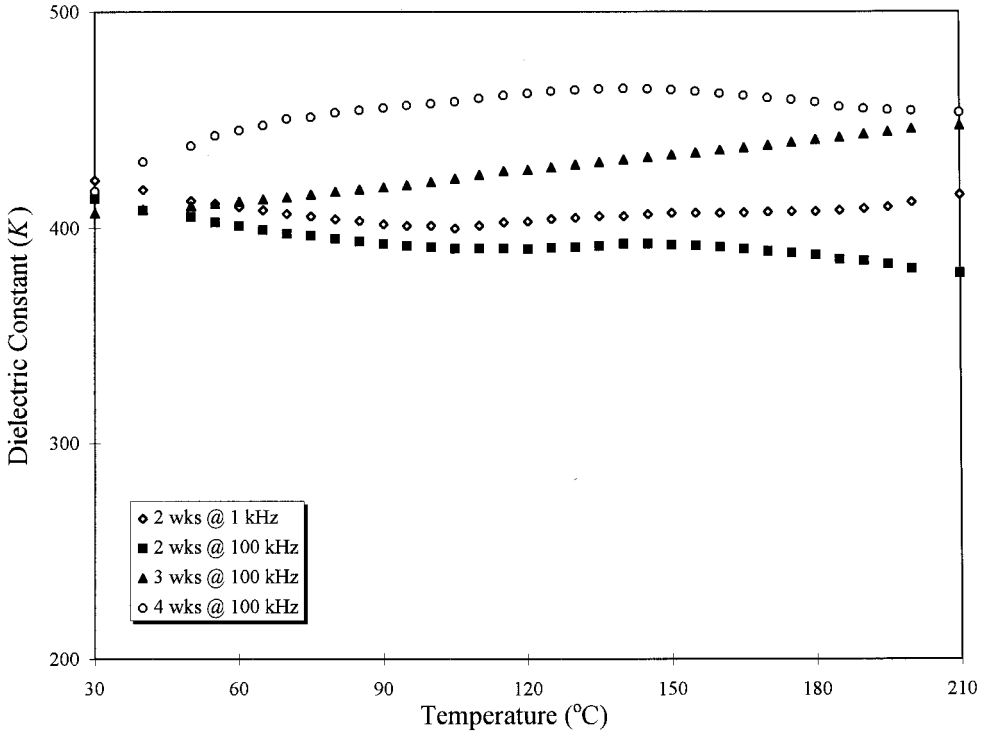

Fig. 8. Dielectric constant (K) of 2-, 3- and 4-week films as functions of temperature at a frequency of 100 kHz, together with that of 2-week film at a frequency of 1 kHz.

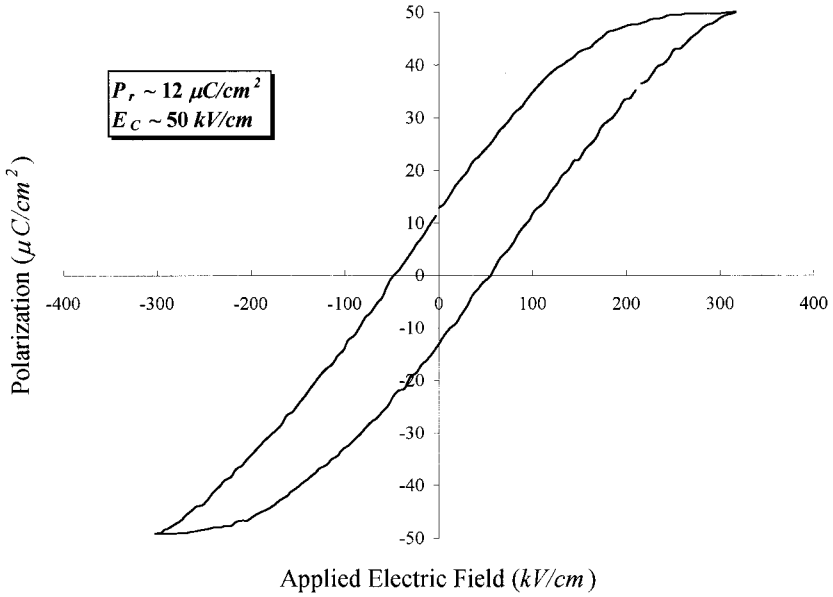

Fig. 9. A typical ferroelectric hysteresis ($P-E$) loop obtained at room temperature of the 3-week film.

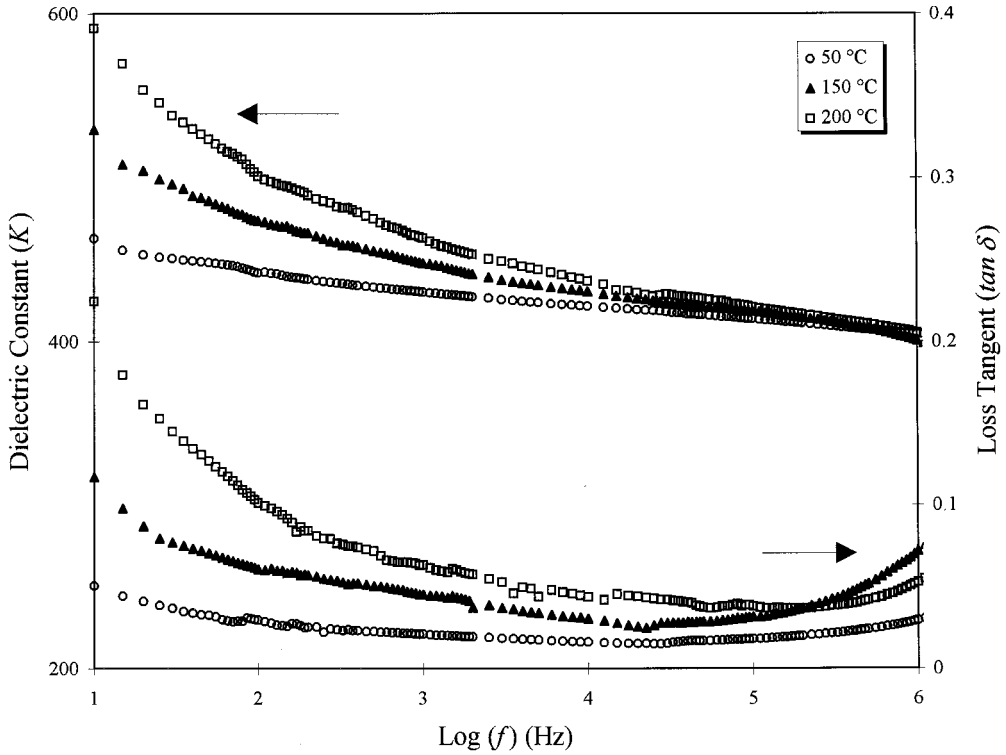

Fig. 10. Dielectric constant (K) and loss tangent ($tan\delta$) of the 3-week $BaTiO_3$ film as function of frequency at temperatures ranging from 50 to 200°C.

temperatures greater than 450°C [15]. In this study, the direct formation of tetragonal films at 240°C was achieved by using optimal levels of hydroxide and chloride ions. The tetragonal symmetry is evidenced by both diffraction and the presence of the characteristic Raman bands of the tetragonal $BaTiO_3$ structure.

B. Electrical Properties

As shown in Figs. 7 and 8, the films synthesized for various times have a dielectric constant around 400–500, which is several times higher than that of the cubic $BaTiO_3$ films synthesized hydrothermally [18–22]. However, there is no clear evidence of a dielectric constant anomaly near the Curie transition as commonly observed in single crystal or ceramic $BaTiO_3$ samples (though a small variation in $tan\delta$ at ~ 120°C was observed in Fig. 7, suggesting a possible Curie transition). The diffusiveness or disappearance of the Curie transition for $BaTiO_3$ thin films has been reported and a variety of mechanisms have been suggested to explain this abnormal behavior, such as a Schottky barrier layer [33,34], defects and microstructural heterogeneity [35], crystalline quality [36], internal and external stress effects [37,38], and the intrinsic size effect [39], as well as depolarization fields that destabilize the ferroelectric phase [40]. In this study, the films have relatively large grain size (around micron range). They are well-crystallized as evidenced by the sharp diffraction peaks with relatively high intensities (Fig. 4), and display a tetragonal symmetry (Figs. 5 and 6). These observations exclude some of the factors mentioned above. With respect to determining whether film stress, Schottky barrier layer and the depolarization fields are causing the absence of the Curie transition in these films, further experiments will be required.

Although there is no dielectric constant anomaly near the Curie transition, the film shows a typical hysteresis $P-E$ loop, indicating its ferroelectric nature. However, the value of $P_r(\sim 12\,\mu C/cm^2)$ obtained for the thin film is lower than that for bulk ceramic $BaTiO_3$, whereas $E_C(\sim 50\,kV/cm)$ is

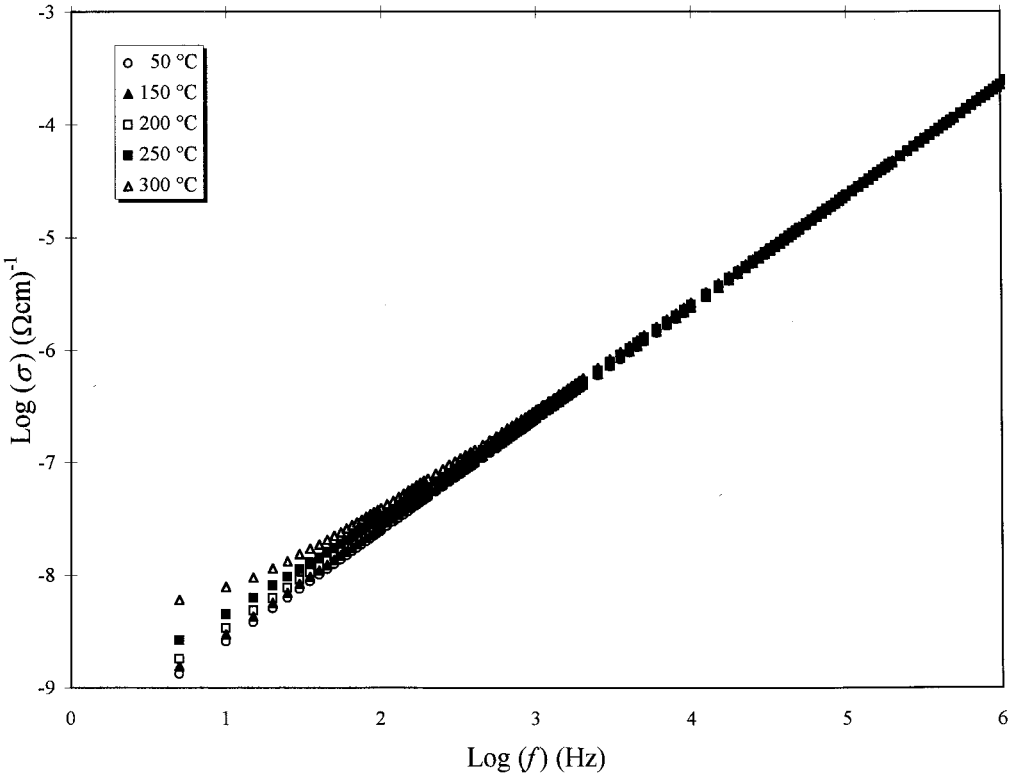

Fig. 11. The ac conductivity of the 3-week film as a function of frequency from 50 to 300°C

considerably greater. Similar values for thin films have been reported and attributed to stress and defects involved in the ferroelectric films [36,37].

The dispersion of K and $tan\delta$ at frequencies below 10^4 Hz (Fig. 10) may be caused by polarization mechanisms that possibly occur at low frequencies [9], including barrier layer polarization, and space charge or interfacial polarization (Maxwell–Wagner type). Each polarization mechanism usually exhibit a relaxation peak in the $tan\delta$ vs. frequency plot. The absence of the peak in Fig. 10 may be attributed to the low-frequency limit of the instrument, which only reveals a partial rise of $tan\delta$ at low frequencies. The apparent temperature dependence of the dispersion indicates that the relaxation mechanism(s) at low frequencies is thermally activated, probably due to the thermally generated free carriers in the film [9].

Conclusions

Well-crystallized tetragonal $BaTiO_3$ thin films were directly produced at 240°C using the hydrothermal synthesis. The microstructure of the films was characterized and their electrical properties examined as functions of temperature and frequency. The formation of the films appears to follow incorporation of Ba^{2+} ions into the hydrated titania on the Ti substrate. Restructuring of the $BaTiO_3$ grains occurs possibly by a dissolution/precipitation mechanism. Thin-film $BaTiO_3$ has a dielectric constant around 400 with no clear indication of the Curie transition, and yet displays a typical ferroelectric hysteresis loop.

Acknowledgments

This work was supported by the National Science Foundation under Grant No. DMR-9202565. The authors would like to thank Dr. C.C. Wang for many helpful discussions and Dr. M. Vitale for helping with the Raman experiments. Suggestions from Profs. P.K. Gallagher, J.J. Lannutti, and Dr. Z. Zhong and Mr. B. Gaskins are also greatly acknowledged.

References

1. P. Li, T.M. Lu, and H. Bakhru, *Appl. Phys. Lett*., **58**, 2639 (1991)
2. M. Okuyama and Y. Hamakawa, *Ferroelectrics*, **63**, 243 (1985).
3. D. Bondurant and F. Gnadinger, *IEEE Spectrum*, **7**, 30 (1989).
4. Y. Yano, K. Iijima, Y. Daitoh, and Y. Bando, *J. Appl. Phys*., **76**, 7833 (1994).
5. O. Auciello, A.I. Kingon, and S.B. Krupanidhi, *Mater. Res. Bull*., **21**(6), 25 (1996).
6. M. De Keijser and G.J.M. Dormans, *Mater. Res. Bull*., **21**(6), 37 (1996).
7. D.L. Kaiser, M.D. Vaudin, G. Gillen, C.S. Hwang, L.H. Robins, and L.D. Rotter, *J. Cryst. Growth*, **137**, 136 (1994).
8. T. Hayashi, N. Ohji, K. Hirohara, T. Fukunaga, and H. Maiwa, *Jpn. J. Appl. Phys*., **32**, 4092 (1993).
9. M.N. Kamalasanan, N.D. Kumar, and S.J. Chandra, *Appl. Phys*., **74**, 5679 (1993).
10. M.H. Frey and D.A. Payne, *Appl. Phys. Lett*., **63**, 2753 (1993).
11. M.N. Kamalasanan, N.D. Kumar, and S. Chandra, *J. Appl. Phys*., **76**, 4603 (1994).
12. M. Yoshimura, S.E. Yoo, M. Hayashi, and N. Ishizawa, *Jpn. J. Appl. Phys*., **28**, L 2007 (1989).
13. N. Ishizawa, H. Banno, M. Hayashi, S.E. Yoo, and M. Yoshimura, *Jpn. J. Appl. Phys*., **29**, 2467 (1990).
14. M. Hayashi, N. Ishizawa, S.E. Yoo, and M. Yoshimura, *J. Ceram. Soc. Jpn*., **98**, 93 (1990).
15. K. Kajiyoshi, N. Ishizawa, and M. Yoshimura, *J. Am. Ceram. Soc*., **74**, 369 (1991).
16. M.E. Pilleux and V.M.J. Fuenzalida, *Appl. Phys*., **74**, 4664 (1993).
17. P. Bendale, S. Venigalla, J.R. Ambrose, E.D. Verink, Jr., and J.H. Adair, *J. Am. Ceram. Soc*., **76**, 2619 (1993).
18. R.R. Bacsa, P. Ravindranathan, and J.P. Dougherty, *J. Mater. Res*., **7**, 423 (1992).
19. R.R. Basca and J.P. Dougherty, *J. Mater. Sci. Lett*., **14**, 600 (1995).
20. E. Shi, C.R. Cho, M.S. Jang, S.Y. Jeong, and H.J. Kim, *J. Mater. Res*., **9**, 2914 (1994).
21. A.T. Chien, J.S. Speck, F.F. Lange, A.C. Daykin, and C.G. Levi, *J. Mater. Res*., **10**, 1784 (1995).
22. K. Osseo-Asare, F.J. Arriagada, and J.H. Adair, *Cer. Tans., Ceramic Powder Sci. IV*, **20**, edited by Messing, G. L., Fuller, Jr., E. R. and Hausner, H. The American Ceramic Society, Westerville, OH, p47, 53 (1988).
23. W. Hertl, *J. Am. Ceram. Soc*., **71**, 879 (1988).
24. N.A. Ovramenko, L.I. Shvets, F.S. Ovcharenko, and B.Y. Komilovich, *Izv. Akad. Nauk SSSR, Neorg. Mater*., **15**, 1982 (1979).
25. P.K. Dutta, R. Asiaie, S.A. Akbar, and W. Zhu, *Chem. Mater*., **6**, 1542 (1994).
26. R. Asiaie, W. Zhu, P.K. Dutta, and S.A. Akbar, *Chem. Mater*., **8**, 226 (1996).
27. M. DiDomenico, Jr., S.H. Wemple, S.P.S. Porto, and R.P. Bauman, *Phys. Rev*., **174**, 522 (1968).
28. G. Burns and B.A. Scott, *Phys. Rev*., **B7**, 3088 (1973).
29. K. Shimomura, T. Tsurumi, Y. Ohba, and M. Daimon, *Jap. J. Appl. Phys*., **30**, 2174 (1991).
30. A.J. Mountvala, *J. Am. Ceram. Soc*., **54**, 544 (1971).
31. C.R. Cho, E. Shi; M.S. Jang, S.Y. Jeong, and S.C. Kim, *Jap. J. Appl. Phys*., **33**, 4984 (1994).
32. J.O. Eckert, C.C. Hung-Houston, B.L. Green, M.M. Lencka, and R.E. Riman, *J. Am. Ceram. Soc*., **79**, 2929 (1996).
33. J.R. Slack and J.C. Burfoot, *J. Phys. C: Solid State Phys*., **4**, 898 (1971).
34. T.R.N. Kutty and P. Padmini, *Mater. Chem. Phys*., **39**, 200 (1995).
35. M.E. Lines and A.M. Glass, *Principles and Applications of Ferroelectrics and Related Materials*, Clarendon Press, Oxford (1977).
36. R.E. Newnham, K.R. Udayakumar, and S.T. Mckinstry, *Chemical Processing of Advanced Materials*, John Wiley & Sons, 379 (1992).
37. S.B. Desu, *Phys. Stat. Solid*., **A141**, 119 (1994).
38. T. Hayashi, N. Ohji, and H. Maiwa, *Jpn. J. Appl. Phys*., **33**, 5277 (1994).
39. S.V. Birykov, V.M. Mukhortov, A.M. Margolin, Y.I. Golovko, I.N. Zakharchenko, V.P. Dudkevich, and E.G. Fesenko, *Ferroelectrics*, **56**, 115 (1984).
40. I.P. Batra, P. Wurfel, and B.D. Silverman, *Phys. Rev*., **8**, 3257 (1973).